



BNL-211431-2019-JAAM

The structures of penicillin-binding protein 4 (PBP4) and PBP5 from Enterococci provide structural insights into beta-lactam resistance

E. D. D'Andrea, A. Soares

To be published in "JOURNAL OF BIOLOGICAL CHEMISTRY"

November 2018

Photon Sciences

Brookhaven National Laboratory

U.S. Department of Energy

USDOE Office of Science (SC), Basic Energy Sciences (BES) (SC-22)

Notice: This manuscript has been authored by employees of Brookhaven Science Associates, LLC under Contract No. DE-SC0012704 with the U.S. Department of Energy. The publisher by accepting the manuscript for publication acknowledges that the United States Government retains a non-exclusive, paid-up, irrevocable, world-wide license to publish or reproduce the published form of this manuscript, or allow others to do so, for United States Government purposes.

DISCLAIMER

This report was prepared as an account of work sponsored by an agency of the United States Government. Neither the United States Government nor any agency thereof, nor any of their employees, nor any of their contractors, subcontractors, or their employees, makes any warranty, express or implied, or assumes any legal liability or responsibility for the accuracy, completeness, or any third party's use or the results of such use of any information, apparatus, product, or process disclosed, or represents that its use would not infringe privately owned rights. Reference herein to any specific commercial product, process, or service by trade name, trademark, manufacturer, or otherwise, does not necessarily constitute or imply its endorsement, recommendation, or favoring by the United States Government or any agency thereof or its contractors or subcontractors. The views and opinions of authors expressed herein do not necessarily state or reflect those of the United States Government or any agency thereof.

The Structures of PBP4fs and PBP5fm from *Enterococcus* provide structural insights into β -lactam resistance

Éverton D. D'Andréa^{1^}, Thomas M. Moon^{1^}, Chris Lee², Alexei Soares³, Jean Jakoncic³, Lou B. Rice⁴, Rebecca Page¹, Wolfgang Peti^{1*}

¹Department of Chemistry and Biochemistry, College of Medicine, University of Arizona, Tucson, AZ; ²Department of Molecular Pharmacology, Physiology and Biotechnology, Brown University, Providence, RI, ³Photon Sciences, Brookhaven National Laboratory, Upton, NY; ⁴Departments of Medicine and Microbiology and Immunology, Warren Alpert School of Medicine of Brown University, Providence, RI

[^]contributed equally

***Corresponding Author:** Wolfgang Peti
University of Arizona
Department of Chemistry and Biochemistry
Tucson, AZ 85721

Phone: (520) 621-3489
E-mail: wolfgangpeti@email.arizona.edu

Abstract:

The final steps of cell-wall biosynthesis in bacteria are carried out by penicillin-binding proteins (PBPs), whose transpeptidase domains form crosslinks in peptidoglycan chains that compose this structure. These enzymes are the targets of β -lactam antibiotics, and their inhibition reduces the structural fidelity of the cell wall. Bacterial resistance to this class of drugs is a growing concern; however, the structural underpinnings of antibiotic resistance derived from the PBPs are not understood. PBP4*fm* and PBP5*fs* have been identified as a low-affinity, class B transpeptidases that confer antibiotic resistance to *Enterococcus faecalis* and *Enterococcus faecium*, respectively. Here, we report the crystal structures of PBP4*fm* and PBP5*fs* in their apo and acyl-enzyme complexes with the β -lactams benzylpenicillin, imipenem and ceftaroline. We find that, although benzylpenicillin, ceftaroline and imipenem adopt similar geometries to that observed in other class B PBP structures, there are small, but significant differences that likely lead to decreased antibiotic efficacy.

Introduction:

'ESKAPE' pathogens (1), including *Staphylococcus aureus*, *Enterococcus faecalis* and *Enterococcus faecium* (the latter two collectively referred to as "enterococci"), are some of the leading causes of nosocomial (hospital acquired) infections (2). In particular, *E. faecium* infections are highly prominent in hospital settings, causing bloodstream, soft tissue and urinary tract infections in compromised patients with indwelling devices (implants) who have been exposed to multiple antibiotics. Unfortunately, treatment of enterococcal infections is significantly compromised by their reduced susceptibility and resistance to most of the commonly employed antimicrobial agents, including aminoglycosides, clindamycin and trimethoprim-sulfamethoxazole (3). Among β -lactam antibiotics, they are resistant to the anti-staphylococcal penicillins and all but one cephalosporin. The three penicillins that have any appreciable activity against enterococci (penicillin, ampicillin and piperacillin) exhibit MICs that are significantly higher than those for the streptococci. Further, rare strains of *E. faecalis* and most nosocomial strains of *E. faecium* exhibit even higher levels of resistance to these penicillins, effectively eliminating β -lactams as a treatment option(1, 2). Finally, enterococci also exhibit tolerance to the bactericidal activity of β -lactams (4), a phenomenon that compromises the use of β -lactam antibiotics as single agents in the treatment of enterococcal endocarditis (5). As a consequence, multi-resistant *E. faecium* and *E. faecalis* represent one of the most dangerous challenges in infectious diseases therapeutics.

The bacterial cell wall, which is composed of layers of peptidoglycan modified with proteins and polymers, is essential for cell survival. In bacteria, this peptidoglycan layer is formed by the coordinated action of multiple proteins, including penicillin-binding proteins (PBPs). PBPs are transpeptidases, carboxypeptidases and endopeptidases that synthesize new and remodel existing peptidoglycan. PBPs are classified by their enzymatic activity: (1) class A, bifunctional PBPs with both glycosyltransferase and transpeptidase activities; (2) class B, transpeptidases; and (3) class C, carboxy-peptidases and endopeptidases. The focus of this study is a subgroup of the class B PBPs, which contain an N-terminal membrane anchoring motif, an N-terminal

extension of unknown function that is hypothesized to mediate protein interactions and a C-terminal transpeptidase (TP) domain.

Reduced susceptibility to β -lactam antibiotics in enterococci results from the expression of a single *low affinity* class B PBP designated PBP4 in *E. faecalis* and PBP5 in *E. faecium*(6, 7)(6, 7)(6, 7)(6, 7). This low-affinity subgroup also includes PBP2a from *S. aureus*, an acquired PBP that confers resistance to many β -lactams (anti-staphylococcal penicillins, most cephalosporins and carbapenems). The PBP active site is located in the TP domain and is defined by three conserved motifs in the TPase domain: *motif I*, which includes the catalytic serine (SxxK: ⁴²⁴STFK^{427/422}STFK⁴²⁵ for PBP4/PBP5); *motif II*, which is involved in the protonation of the β -lactam leaving group (S/YxN; ⁴⁸²SDN^{484/480}SDN⁴⁸²); and *motif III* which facilitates substrate binding and defines the oxyanion hole (K[T/S]GT; ⁶¹⁹KTGT^{622/617}KTGT⁶²⁰) (**Fig. 1A**). The nucleophilic serine (Ser424/Ser422 for PBP4/PBP5) is located at the N-terminus of helix α 2 while oxyanion hole is defined by the backbone nitrogens of the nucleophilic serine and the motif III threonine (Thr622/Thr620). These motifs are bordered above by the 'lid' (aa 445-473/443-471 for PBP4/PBP5) and below by the C-terminal helix (aa 657-680/655-678) which together enclose the active site in a deep cleft.

In class B PBP transpeptidases, the catalytic serine attacks the carbonyl of the penultimate D-Ala residue of a 'donor' stem peptide, releasing the C-terminal D-Ala and forming a covalent acyl-enzyme adduct with the donor peptide. In a second step, the carbonyl of D-Ala adduct undergoes nucleophilic attack from a primary amine located at the extremity of a side chain of an acceptor stem peptide. This creates a bridge between the peptides and, in turn, links the glycan strands to which they are attached. β -lactams (penicillins, carbapenems, monobactams and cephalosporins) mimic the D-Ala-D-Ala sequence in the donor substrate and function as suicide inhibitors. Since their discovery as the targets of β -lactam antibiotics, PBPs have been the subject of intense research especially regarding their role in the resistance to β -lactams of both *S. aureus* and *enterococci*.

Because these PBPs have unusually low affinities for β -lactams, the β -lactam acylation rates are negligible compared with bacterial generation times, allowing the pathogens to survive antibiotic treatment. Of greater concern is the observation that prolonged β -lactam therapy can lead to the emergence of highly resistant strains. In *E. faecium*, high-level resistance correlates with mutations in the PBP5 catalytic domain that weaken further affinities for β -lactams (8)(8). While elevated resistance in *E. faecalis* strains are comparatively rarer, they have similarly emerged after prolonged β -lactam treatments with the increased resistance, often due to mutations in PBP4(9).

Despite their clear biological and translational importance, only a handful of publications have reported fundamental molecular insights on *E. faecalis* PBP4 or *E. faecium* PBP5 activity, structure and function, limiting progress in the field for nearly two decades. Here, we determined the structures of PBP5 and PBP4 both alone and bound to multiple antibiotics. Our structures reveal that, like PBP2a from *S. aureus*, the catalytic serine adopts a conformation poorly positioned for nucleophilic attack. Together, our studies are defining the subtle functional and structural difference in the enterococci PBPs that allow them to both support transpeptidase activity while also being resistance to antibiotics that function and substrate mimics.

RESULTS

PBP4 is the sole loci responsible for reduced β -lactam susceptibility in *E. faecalis*

Prior studies describing deletion of *pbp5* from the *E. faecium* genome and *pbp4* from the *E. faecalis* genome have implicated PBP5 and PBP4 as the sole loci responsible for reduced penicillin susceptibility and cephalosporin resistance in clinical enterococcal strains (1, 2). Complementation studies in *E. faecium* have confirmed the involvement of PBP5 in resistance and detailed the role of different amino acid substitutions in higher levels of resistance (3). Here, we performed similar complementation experiments in *E. faecalis* with *pbp4* expressed from shuttle plasmid pBSU101 (4) in *pbp4*-deletion mutant JH2-2(Δ PBP4)(1). The data show that deletion of *pbp4* from *E. faecalis* JH2-2 resulted in an increased sensitivity to five different β -lactam antibiotics (**Table 1**). The most striking increase in β -lactam sensitivity (measured as a reduction in MIC) was observed for ceftriaxone, whose MIC was reduced from >100 μ g/ml to 0.39 μ g/ml. Ceftaroline also had a substantial reduction from 3.13 μ g/ml to <0.098 μ g/ml. MICs for ampicillin, penicillin and imipenem were less affected, reflecting the intrinsic activity of these agents against PBP4. Re-introduction of *pbp4* on a plasmid was associated with a return of resistance. The active β -lactams were somewhat less active than versus JH2-2, presumably reflecting the 19.8-fold increase in expression from the plasmid compared to the chromosomal expression in JH2-2 (Supplemental Figure). Together, the data show that *pbp4* is the sole loci responsible for reduced β -lactam susceptibility in *E. faecalis*.

PBP4 from *E. faecalis* adopts a structure similar to PBP5_{fm}

We used X-ray crystallography to determine the structures of PBP4_{fs} (*E. faecalis* PBP4₃₆₋₆₈₀, which lacks the N-terminal membrane anchor; hereafter referred to as PBP4) and PBP5_{fm} (*E. faecium* PBP5₃₇₋₆₇₈, which also lacks the N-terminal membrane anchor; hereafter referred to as PBP5) (**Table 2**). We obtained two different crystal forms of PBP5, which allowed us to determine the structures of PBP5 in two distinct conformations (open and closed) to resolutions of 2.7 Å and

2.9 Å, respectively (**Fig. 2A**). Strong electron density was observed for the entire sequence with the exception of 3 loops for the open conformation (140-144, 246-249, 625-630). The structure of PBP4 was determined to 1.8 Å resolution. Strong electron density was observed for residues 172-680; interpretable electron density was not observed for the N1 domain and 3 short loops (**Fig. 2B**). The structures show that both PBPs are composed of four distinct structural domains: two N-terminal domains (N1 and N2), a non-penicillin binding domain (nPB) and a C-terminal catalytic transpeptidase (TPase) domain, which contains the nucleophilic serine (**Figs. 2A,B**). With the exception of the N2 domain, all domains are comprised of residues that are not linear in sequence giving rise to an extensively interconnected topology (**Fig. 2C**; residues numbers for PBP5: N1, 43-171/314-339; N2, 192-258; nPB, 172-191/259-313/340-348/384-409; TPase, 349-383/410-678).

The PBP identified to be most similar to PBP4 is PBP5 (determined using the DALI structural homology server; Z-score of 62.5; sequence identity of 60%), with the individual domains of both proteins superimposing with root mean square deviations of 0.75 -1.1 Å (**Table S1**). The largest differences are observed in the TPase domain (structural elements that brace one side of the active site are shifted by 1.5 – 2.0 Å in PBP4 due to the presence of a tyrosine in PBP4, Tyr605, which, in PBP5, is a much smaller threonine residue, Thr603) (**Fig. S1B**). The next most similar PBP is PBP2a from *S. aureus* (hereafter referred to as PBP2a; Z-scores of 49.3 and 51.0 and sequence identities of 41% and 38% for PBP4 and PBP5 versus PBP2a, respectively), whose TP domain aligns with those of PBP4 and PBP5 with > 2.0 Å rmsd. Together, these proteins represent the defining members of the low affinity, high molecular weight, class B PBPs.

The N1 and N2 domains are highly dynamic, rotating as rigid bodies independently of the TPase domain.

Overlaying the three members of this family (PBP4, PBP5_{open}, PBP5_{closed}, PBP2a) on the TPase domain reveals that the N1 and N2 domains are dynamic, adopting a wide range of

conformations relative to the TPase domain. In particular, to transform the PBP5*closed* to the PBP5*open* state, the N1 and N2 domains must rotate by 44° and 39°, respectively, which widens the cleft between the N1 and N2 domains from 7 Å (closed) to 31 Å (open; **Fig. 2A**). The dynamic nature of the N1 domain was confirmed by our structure of PBP4. Namely, no interpretable electron density was observed for the PBP4 N1 domain, suggesting it adopts multiple conformations in the crystal. Finally, the N1 domain of PBP2a adopts a third conformation, with 75° and 88° rotations relative to those of PBP5*open* and PBP5*closed*, respectively. Similar observations were made for the N2 domain, in which all four N2 domains (PBP4, PBP5*open*, PBP5*closed* and PBP2a) adopt distinct orientations and are related to one another by rotations of 39°-52° (**Fig. 3A, S1A**).

The function of the N-terminal domains in this family of HMW Class B PBPs is still under debate, with some suggesting they function as protein-protein interaction domains and others suggesting they function as molecular 'spacers', forcing the catalytic site to remain a certain distance from the membrane. We used the DALI structural homology server in order to identify those proteins that are most similar to the N1 and N2 domains, in order to gain insights into the degree of conservation, and the potential function of these domains. The data revealed that the N-terminal domains are differentially conserved within the larger PBP family. While the N1 domain (PBP5) is only found in PBP2a (*S. aureus*; Z-score, 17.7), the N2 domain (PBP5 and PBP4) are found in PBP2a (*S. aureus*; Z-score, 10.0), PBP3 (*P. aeruginosa*; Z-score, 7.3) and PBP1 (*S. aureus*; Z-score, 6.6). Unexpectedly, they were also shown to be structurally similar to proteins outside the PBP5 family. Namely, the N1 domain was identified as being similar to ketosteroid isomerase domains (Z-score, 12.9; **Fig. S1C**), while the N2 domain was identified as being similar to the ATP-dependent CLP protease adaptor protein CLPS2 (Z-score, 5.9; **Fig. S1D**). These latter observations are consistent with the hypothesis that the class B PBP N-terminal domains function as protein interaction domains. The proteins that interact directly with the N1 and N2 domains from PBP4, PBP5 and PBP2a are still unknown.

Conformational changes associated with β -lactams acylation are localized to the catalytic site.

Previous studies of methicillin-resistant PBP2a showed that PBP2a motif III (β -strand β 3) is twisted relative to the methicillin-susceptible PBP2, resulting in the carbonyl residue of the last 'T' residue in the K[T/S]GT motif angled towards the oxyanion hole. Further β -lactam acylation showed that this results in a twist of strand β 3, allowing the β -lactam carbonyl to point directly into the oxyanion hole. Together, these data suggested that the slow acylation rate of PBP2a may be due to this distorted conformation of β 3.

Like PBP2a, the β -lactam resistance of PBP5 and PBP4 has also been shown to be due to the inefficient formation of the acyl-PBP intermediate. In order to understand the molecular basis of PBP4 and PBP5 resistance to β -lactams, we determined the structures of five distinct acyl-enzyme complexes: PBP4:benzylpenicillin, PBP4:imipenem, PBP4:ceftaroline, PBP5:benzylpenicillin and PBP5:imipenem, representing three different β -lactam classes (*penicillins*, penG; *carbapenems*, imipenem; *cephalosporins*, ceftaroline). Examination of the active sites revealed strong density for all covalent acyl-enzyme adducts (**Figs. 4A-4C**). As observed for PBP2a, superposition of the apo and β -lactam bound structures revealed that adduct formation does not result in global conformational changes in either PBP5 or PBP4, as the RMSDs between the apo- and the drug-bound transpeptidase domains are between 0.31 and 0.53 Å (**Table S2**). Rather, the changes are localized to domain movements about the active site and changes in the structures of the active site motifs. However, as described below, the changes are not identical between the free and β -lactam bound structures, but instead are dependent upon the particular acyl-adduct formed. Because the differences observed between apo-PBP4 versus β -lactam-acyl-PBP4 and apo-PBP5 versus β -lactam-acyl-PBP5 are essentially identical for benzylpenicillin and imipenem; the PBP4 β -lactam complexes are described here.

Penicillins: Benzylpenicillin acylation induces a rotation of the nucleophilic serine and a twist of strand β 3.

As expected, the benzylpenicillin forms a covalent adduct with PBP4 via its catalytic serine, Ser424. The electron density is well-defined for the entire molecule (**Fig. 4A**), with the benzylpenicillin carbonyl oxygen pointing towards the oxyanion hole defined by the backbone nitrogens of Ser424 and Thr622 (**Fig. 4D**). The benzylpenicillin is further stabilized by polar contacts with both PBP4 backbone atoms and the sidechains of Ser482, Asn484, Lys619, Thr620 and Thr622; Lys427 forms intraprotein polar contacts with Asn484 and Ser482 to further stabilize the acylated active site configuration.

The PBP4 apo and benzylpenicillin-acyl-PBP complex structure reveals that, like PBP2a, it has a distorted active site that undergoes both local and distributed conformational changes upon β -lactam acylation (**Fig. 4E**). First, in apo-PBP4, the nucleophilic Ser424 hydroxyl points down towards the oxyanion catalytic pocket. However, upon acylation with benzylpenicillin, the C β -O γ bond rotates by $\sim 150^\circ$. As a consequence, O γ moves by 1.3 Å, and, in the acylated complex, is now orientated away from the oxyanion hole. Although this conformational change differs from that observed for Ser403 in PBP2a, which results in a shift but not a rotation of the nucleophilic hydroxyl, it does suggest that the serine side chain is not ideally positioned for nucleophilic attack in the apo conformation. Because the β -lactam carbonyl now points towards the oxyanion hole, it displaces the carbonyl of Thr622, which rotates out of the hole and upwards towards the bound β -lactam moiety (**Fig. 4E**). This rotation of strand β 3 results in the formation of two additional hydrogen bonds: (1) the first between the β -lactam carbonyl and the amide hydrogen of Thr622 and (2) the second between the phenylacetyl nitrogen and the Thr620 sidechain hydroxyl. Finally, the Thr618 sidechain adopts a rotamer conformation that expands the active site in order to accommodate the β -lactam phenyl ring. The conformation of benzylpenicillin in the PBP4:benzylpenicillin complex is similar to other benzylpenicillin-bound PBP structures, with the exception that the phenylacetyl group is observed in some structures to

be rotated upwards away from motif III. Finally, because the catalytic site of PBP4 is located in a deep, narrow cleft (**Fig. 4E**), the structural elements that enclose the catalytic site open in order to accommodate benzylpenicillin acylation. This results in a displacement of the 'lid' moiety by 1.9 Å for penG-acyl-PBP4 compared to its apo- conformation (**Fig. 4E**).

Carbapenems: imipenem acylation does not alter the twist of strand β 3.

Imipenem also forms a covalent adduct with Ser424 and its electron density is well ordered for the entire molecule with the exception of its iminomethyl-amino tail (**Fig. 4B**). Overall, imipenem binds PBP4 in a manner similar to that observed in the benzylpenicillin-acyl-PBP complex; however, there are also distinct differences. As observed in the benzylpenicillin-acyl-PBP4 complex, the side chain of Ser424 rotates out of the oxyanion hole to form the acyl-enzyme adduct (**Fig. 4F**). However, unlike in benzylpenicillin, where the β -lactam carbonyl points downward into the oxyanion hole, the imipenem carbonyl points upward, away from the oxyanion hole where it hydrogen bonds with Lys427 and residue Asn484 (**Fig. 4F**). Because of this, the carbonyl of motif III Thr622 does not rotate out of the oxyanion hole, but instead retains the twisted conformation of β 3 it adopts in the apo- conformation (**Fig. 4G**). Additional polar contacts are observed between imipenem and the backbone and/or sidechain atoms of Ser482, Thr620 and Thr622. The conformations of imipenem bound to PBP4 and PBP5 are essentially identical both to one another and other imipenem-transpeptidase complexes, with the exception that the iminomethyl-amino tail adopts a wide range of conformations, an observation consistent with a lack of strong electron density for this element. Finally, as observed for benzylpenicillin, both the lid and central β -sheet open to accommodate imipenem acylation; however, they do so to a far less extent than that observed for benzylpenicillin, with the lid moving by only 0.7 Å (**Fig. 4G**).

Cephalosporins: Ceftaroline acylation results in the widest opening of the catalytic cleft.

We also determined the structure of the ceftaroline-acyl-PBP4 complex (**Fig. 4C**). Although the related PBP2a complex has been proposed to bind two molecules of ceftaroline (one forming the acyl-enzyme complex and a second molecule binding at a putative allosteric site located between the N1 and nBP domains), we observed density for only a single ceftaroline molecule in PBP4. The ceftaroline carbonyl oxygen points towards the oxyanion hole defined by the backbone nitrogens of Ser424 and Thr622 (**Fig. 4H**). Ceftaroline is further stabilized by multiple polar interactions with the sidechains of Ser482, Asn484, Lys619 and Thr620 and the backbone atoms of Gly541 and Thr622 and intraprotein polar interactions between Lys427, Ser482, Asn484 and Lys619.

The differences between PBP4 and ceftaroline-acyl-PBP4 adduct are most similar to the adduct formed with benzylpenicillin complex than that with imipenem. First, as observed for both benzylpenicillin and imipenem, ceftaroline acylation results in a rotation of the nucleophilic serine upwards away from the oxyanion hole (**Fig. 4I**). However, as observed for benzylpenicillin, acylation of PBP4 by ceftaroline displaces the Thr622 carbonyl out of the oxyanion hole, causing strand β 3 to twist outward. This new orientation of the Thr622 carbonyl is stabilized by the acetylamino nitrogen, which forms a hydrogen bond with the Thr622 carbonyl. An identical polar interaction is present in the penG-acyl-PBP4 complex between the benzylpenicillin phenylacetyl nitrogen and the Thr622 carbonyl. In contrast, imipenem lacks a nitrogen in the corresponding position, explaining why the imipenem-acyl-PBP complex does not result in a rotation of strand β 3. Finally, ceftaroline results in the greatest opening of the catalytic cleft, with the lid and central β -sheet both moving by ~ 2.7 Å to accommodate ceftaroline binding (**Fig. 4I**).

β -lactam acylation does not increase PBP4 and PBP5 thermal stability.

To determine if β -lactam acylation increases PBP4 and PBP5 stability, we used differential scanning fluorimetry (DSF). We first compared the melting temperatures (T_{ms}) of free PBP4 and PBP. The DSF data show that they unfold at similar temperatures, with T_{ms} of 54.5 °C and 53.2

°C for PBP4 and PBP5, respectively (**Table 3**). We then incubated both PBPs with either benzylpenicillin, imipenem or ceftaroline for either 1 or 12 hours and repeated the DSF measurements. The data show that all three β -lactams alter the PBP T_m s and do so in a manner that depends on both the β -lactam and the PBP protein. First, imipenem modestly increases the T_m of both PBP4 and PBP5, with the largest increase observed for PBP4 and a 12 hr incubation ($\Delta T_m +1.8$ °C), suggesting it slightly stabilizes the conformation of both PBPs. In contrast, while benzylpenicillin results in an increase in the PBP5 T_m (up to $\Delta T_m +1.8$ °C at a 12 hr incubation), it decreases the T_m for PBP4 (-0.8 °C for the 1 hr incubation). This suggests acylation by benzylpenicillin slightly increases the stability of PBP5 while it has the opposite effect, decreasing the stability, on PBP4. The largest differences in T_m s between the apo and acylated PBPs were observed with ceftaroline (between -2.0 to 4.2 °C). Further, while ceftaroline destabilized PBP4 ($\Delta T_m -3.7$ °C for 1 hr incubation), it stabilized PBP5 ($\Delta T_m +4.2$ °C for 12 hr incubation). Taken together, the data show that both benzylpenicillin and imipenem have measurable, but modest effects on the T_m s of both PBP4 and PBP5, while ceftaroline has much larger effects, consistent with the larger conformational changes observed between PBP4 and the ceftaroline-acyl-PBP4 adduct.

Discussion

PBP4, PBP5 and PBP2a are the defining members of the low affinity high molecular weight class B PBPs. The availability of the 3-dimensional structures of all three PBPs in multiple states provides a unique opportunity to define the structural and functional similarities and differences within this family and how this impacts their ability to be inhibited by β -lactams. As observed for other PBPs, β -lactam binding to PBP4 and PBP5 does not lead to extensive conformational changes; rather the changes are exclusively localized to and around the catalytic pocket. The conformations observed both in the apo- and β -lactam bound states are similar for all members

of the low affinity class B high molecular PBPs (i.e., PBP4, PBP5 and PBP2a). Namely, as observed for apo-PBP2a, similarly the catalytic serine of PBP4 and PBP5 is not ideally positioned for nucleophilic attack. Further, strand $\beta 3$ is twisted towards that catalytic pocket, with the PBP4 Thr622 carbonyl (PBP5, Thr620) pointing towards the oxyanion hole. As observed for PBP2a upon acylation with nitrocefin, the catalytic serines of both PBP4 and PBP5 rotate upward upon acylation with benzylpenicillin (PBP4/PBP5) or ceftaroline (PBP4), while strand $\beta 3$ rotates upward moving the PBP4 Thr622 (PBP5 Thr620) carbonyl out of the oxyanion hole. However, this is only observed for a subset of β -lactams, as it is surprisingly not observed when either PBP4 or PBP5 are acylated with imipenem. Although the unusual twisted conformation of strand $\beta 3$ (and its rotation upon acylation with a subset of β -lactams) was originally identified in PBP2a, and now in PBP4 and PBP5, it has also been identified in a number of other PBPs, including PBP_a from *M. tuberculosis* and PBP2_x from *S. pneumoniae*. Further, the observation in PBP4 and PBP5 that the rotation of strand $\beta 3$ upon β -lactam acylation depends on the nature of the β -lactam is also observed in PBP2_x with strand $\beta 3$ rotating upon acylation with benzylpenicillin but remaining in a twisted conformation upon acylation with imipenem, i.e., identical to which is observed for PBP4 and PBP5. The second major conformational change associated with β -lactam acylation is a widening of the catalytic cleft to accommodate both β -lactams and substrates. PBP4 and PBP5, in particular, are characterized by an unusually deep catalytic pocket that is bounded by structural elements, especially the lid that braces the top of the catalytic pocket that must open in order for β -lactams (and substrates) to access the catalytic serine. Once acylated, these elements maintain a more open conformation due to the presence of the β -lactam, from between 0.7 – 2.7 Å, depending on the bound β -lactam. This widening of the catalytic cleft is routinely observed those PBPs whose structures have been determined with and without β -lactam acylation.

Kinetic and structural studies have suggested that one member of this family, PBP2_a, contains an allosteric pocket at the N1-nBP junction that, when occupied, biases the conformation of the PBP2_a active site towards a state that is more susceptible to ceftaroline acylation, a model

that is still controversial. Our discovery that the N1 and N2 domains rotate independently of the TP domain and do not alter the conformation of the catalytic site suggests that PBP4 and PBP5 are not regulated by allostery. This was confirmed by our structures which showed that all β -lactams tested bind PBP4 and PBP5 with 1:1 stoichiometries, forming acyl-enzyme complexes with the catalytic serine. Further, overlaying our PBP5 structures with that of PBP2a bound to the putative allosteric ceftaroline demonstrates that, both in the open and closed PBP5 conformations a corresponding allosteric binding pocket is not present. This is because, in PBP5, the short nBP α -helix clashes with the ceftaroline molecule. Finally, the few PBP2a residues that contact the non-covalently bound ceftaroline are not conserved in either PBP4 or PBP5. Together, our data show that PBP4 and PBP5 do not contain an allosteric binding pocket and instead bind ceftaroline in a 1:1 ratio. Further, in spite of these domains being highly interconnected (**Fig. 2C**), our data show that these domains are independent, likely adopting a wide range of relative orientations in the cell, making allosteric communication with the active site difficult.

Finally, although modest conformational changes in the N-terminal domains have been observed in other PBPs, our structures demonstrate that large rigid body rotations of both the N1 and N2 domains are readily accessible in this family of proteins. In particular, our structures of an open and closed state of PBP5 reveal that the N1-N2 interdomain distance can change by more than 24 Å. More importantly, these structures show that these rotations occur without altering the conformation between domains, as the nBP and TP domains of the open and closed states superimpose on one another with RMSDs less than 0.25 Å. This demonstrates that, in the periplasm, the N1 and N2 domains of PBPs in this family are likely dynamic, rotating as rigid bodies relative to the nBP and TP domains. Although the function of these domains is currently unknown, they are hypothesized to mediate protein:protein interactions in the periplasm, a hypothesis consistent with the discovery that these domains are most similar to a ketosteroid isomerase (N1) and CLPS adaptor protein (N2).

Methods:

Complementation of *pbp4* in *E. faecalis* *pbp4*-deletion mutant JH2-2(Δ PBP4)

pbp4 was amplified from *E. faecalis* JH2-2 (including the 200 bp upstream of the structural gene; native promoter) and ligated to pBSU101 after removal of the pBSU101 native promoter and *gfp* gene. This plasmid construct was then introduced by electroporation into *E. coli* DH10B. Successful transformation was confirmed by plasmid extraction and restriction digestion, along with PCR amplification and sequencing of *pbp4* within the plasmid. The final plasmid (pRIH304) was then transformed into *E. faecalis* JH2-2(Δ *pbp4*) by electroporation (spectinomycin selection; 125 μ g/ml). Expression of PBP4 was confirmed by Western Blot using a polyclonal anti-PBP4 antibody as previously described (Supplemental Figure X)(5).

Cloning and Expression of PBP4_{fc} and PBP5_{fm}

E. faecalis PBP4 (36-680) and *E. faecium* PBP5 (37-678), which lack the N-terminal transmembrane domains, were subcloned into the pRP1b expression vector encoding an N-terminal His₆-tag and a TEV cleavage site (ref) and expressed in *E. coli* BL21 (DE3) cells. Cells were grown in Luria Broth in the presence of selective antibiotics at 37 °C up to OD₆₀₀ of 0.8 - 1.0 and expression was induced by the addition of isopropyl- β -D-1-thiogalactopyranoside (IPTG), 1.0 mM and 0.5 mM for PBP5 and PBP4 respectively. Proteins were expressed for ~18 hours at 18 °C prior to harvesting by centrifugation at 8,000 x *g* for 55 minutes at 4 °C. Bacterial pellets were used immediately or stored at -80 °C. For purification, cell pellets were resuspended in lysis buffer (50 mM Tris pH 8.5, 500 mM NaCl, 5 mM imidazole, 0.1 % Triton X-100) and lysed using high pressure homogenization (Avestin EmulsiFlex C3). The cell lysate was centrifuged at 42,500 x *g* for 55 minutes at 4 °C. The clarified supernatant loaded onto a pre-equilibrated HisTrap HP column (GE) and eluted using an imidazole gradient. The fractions containing the PBP (PBP4 or PBP5) were pooled and dialyzed for 48 hours at 4 °C with TEV protease to remove the N-terminal His₆-tag. A second Ni-NTA purification step was used to remove the cleaved His₆-tag, any

remaining uncleaved protein and the His₆-tagged protease. The cleaved PBP4 and PBP5 were then dialyzed for 3 hrs at 20 °C against 10 mM Tris pH 8.0, 1.5 M (NH₄)₂SO₄, after which they were loaded onto a pre-equilibrated HiTrap Phenyl HP hydrophobic interaction column (GE Healthcare). Fractions containing the PBP were pooled, dialyzed against SEC buffer (10 mM Tris pH 8.5 and 300 mM NaCl [PBP4] or 800 mM NaCl [PBP5]) for 3 hours at 20 °C and purified using size exclusion chromatography (SEC; Superdex 200 26/60; GE healthcare). The resulting monomeric peaks were pooled and concentrated to 12 mg/mL (PBP4) or 15 mg/mL (PBP5).

Crystallization

PBP4. Purified PBP4 crystallized in 40 mM KH₂PO₄ pH 3.25, 16% PEG 8000, 20% glycerol, 10 mM TCEP (vapor diffusion). PBP4 acylated complexes with benzylpenicillin, imipenem, and ceftaroline were obtained by soaking PBP4 crystals with a 40-fold molar excess of the β -lactam for 45 minutes (benzylpenicillin) or 1 hour (imipenem/ceftaroline); crystals used for soaking were grown in the same condition that for apo PBP4 with the exception that the TCEP was eliminated and, for the benzylpenicillin-acyl-PBP4 complex, the crystals were grown in 24% glycerol. PBP4 *apo* and complex crystals were harvested directly from the well and immediately flash frozen in liquid nitrogen. *PBP5, open state*. The open state of PBP5 crystallized in 0.1 M tri-sodium citrate pH 5.5, 2.0 M ammonium sulfate (vapor diffusion). The penicillin-acyl-PBP5 complex was obtained using co-crystallization using the same condition, but also including a 20-fold molar excess of benzylpenicillin. The imipenem-acyl-PBP5 complex was obtained by soaking PBP5 crystals in crystallization buffer supplemented with a 20-fold molar excess of imipenem for 12 hours. PBP5 *apo* and β -lactam acylated complexes were cryoprotected using 5.0 M ammonium sulfate after which they were immediately flash frozen in liquid nitrogen. *PBP5, closed state*. Crystals were obtained using the acoustic droplet ejection (ADE) robot at NSLSII in 100 mM BisTris pH 6.5, 7.5% (w/v) PEG3350, 7.5% (v/v) PEG400, 25 mM sucrose, 25 mM trehalose, 25 mM glucose and 25 mM galactose.

Data collection, processing and solution

Data were collected at SSRL (beamline 12-2; PBP5, open state, benzylpenicillin-acyl-PBP5, imipenem-acyl-PBP4 and ceftaroline-acyl-PBP4), APS (beamline 23ID; imipenem-acyl-PBP5) or the University of Arizona (Bruker liquid Gallium MetalJet with a Photon II CPAD detector; PBP4, benzylpenicillin-acyl-PBP4). Data were processed using either AutoXDS, XDS or SAINT/XPREP. The open state of PBP5 and PBP4 were both phased using molecular replacement (MR, PHASER as implemented in Phenix), using PDBID 5DVY as a search model. The closed state of PBP5 was phased using MR (same programs) but using the PBP5 closed state as a search model. The β -lactam-acyl-PBP complexes were phased using either MR or difference Fourier methods. Clear electron density was visible for all acylated β -lactams. All structures were completed using iterative rounds of manual building (Coot) and refinement (Phenix). Molecular figures were generated using PyMOL.

Differential Scanning Fluorimetry

Purified PBP4 and PBP5 either alone or in the presence of either a 40-fold (PBP4) or 20-fold (PBP5) molar excess of benzylpenicillin, imipenem, and ceftaroline were incubated for 1 hour or overnight. Forty-five microliters of each protein at a concentration of 1.1 mg/ml was added to 5 μ L of 20x SYPRO (5000X, Invitrogen) for a final reaction volume of 50 μ L. DSF experiments were performed on a CFX96 touch RT-PCR System (Bio-Rad); temperature was ramped from 4 $^{\circ}$ C to 80 $^{\circ}$ C in 0.2 $^{\circ}$ C increments (5 seconds each increment). Data were analyzed with the Bio-Rad CFX manager 3.1 software and SigmaPlot.

Tables

Table 1: Minimal Inhibitory concentrations for different -lactam antibiotics against *E. faecalis* strains

Strain	MIC ($\mu\text{g}/\text{mL}$)				
	Ampicillin	Penicillin	Ceftriaxone	Imipenem	Ceftaroline
JH2-2	0.78	1.56	>100	0.78	3.13
JH2-2 ΔPBP4	0.39	0.78	0.39	0.39	<0.098
LS304*	1.56	6.25	>100	3.13	6.25

**LS304 is JH2-2PBP4 transformed by plasmid p*

Table 2: Data collection and refinement statistics

	PBP5 <i>open</i>	PBP5 <i>closed</i>	PBP5 + benzylpenicillin	PBP5 + imipenem
Data collection				
Space group	P6 ₃ 22	P4 ₃ 2 ₁ 2	P6 ₃ 22	P6 ₃ 22
Cell dimensions				
a, b, c (Å)	190.5, 190.5, 156.5	62.7, 62.7, 371.2	192.3, 192.3, 156.1	192.9, 192.9, 155.9
α, β, γ (°)	90, 90, 120	90, 90, 90	90, 90, 120	90, 90, 120
Resolution (Å)	39.5 - 2.70 (2.79 - 2.70) ^a	30.0 - 2.86 (2.86 - 2.94) ^a	39.0 - 2.93 (3.06 - 2.93) ^a	29.8 - 2.80 (2.91 - 2.80)
<i>R</i> _{merge}	0.059 (0.445)	0.152 (0.575)	0.255 (2.78)	0.157 (1.66)
<i>I</i> /σ(<i>I</i>)	13.0 (2.5)	12.7 (3.0)	9.2 (1.7)	20.1 (1.8)
<i>CC</i> _{1/2}	0.997 (0.707)	0.997 (0.778)	0.991 (0.379)	0.999 (0.337)
Completeness	0.99 (0.98)	0.99 (0.91)	0.99 (0.98)	0.99 (0.99)
Redundancy	3.1 (3.2)	12.9 (9.9)	7.5 (7.5)	18.3 (12.9)
Refinement				
Resolution (Å)	39.5 - 2.7	29.7 - 2.9	39.0 - 2.9	29.8 - 2.8
Unique reflections	45726	18016	36572	42395
<i>R</i> _{work} / <i>R</i> _{free}	0.18/0.21	0.22/0.28	0.19/0.21	0.17/0.19
No. atoms	4874	4478	4880	5057
Protein	4664	4473	4726	4798
Ligand/ion	85	-	115	95
Water	125	5	39	164
<i>B</i> factors				
Protein	56.7	57.6	63.5	76.6
Ligand/ion	95.9	-	101.8	105.9
Water	50.0	38.3	45.8	68.6
R.m.s. deviations				
Bond lengths (Å)	0.003	0.002	0.002	0.003
Bond angles (°)	0.558	0.497	0.453	0.574
PDB ID				

^a Values in parentheses are for highest-resolution shell.

Table 2: Data collection and refinement statistics continued

	PBP4 <i>apo</i>	PBP4 + benzylpenicillin	PBP4 + imipenem	PBP4 + ceftaroline
Data collection				
Space group	C2	C2	C2	C2
Cell dimensions				
a, b, c (Å)	124.7, 84.6, 85.1	123.3, 85.5, 83.7	123.8, 85.4, 84.6	123.5, 85.5, 82.7
α , β , γ (°)	90, 109.3, 90	90, 109.5, 90	90, 110.3, 90	90, 109.9, 90
Resolution (Å)	17.5 – 1.80 (1.83 – 1.80) ^a	17.7 – 2.34 (2.38 – 2.34)	37.9 – 2.62 (2.74 – 2.62)	39.0 – 2.98 (3.17 – 2.98)
R_{merge}	0.072 (0.430)	0.162 (0.606)	0.058 (0.211)	0.136 (0.396)
$I/\sigma(I)$	16.5 (2.5)	9.4 (2.1)	12.5 (3.7)	5.4 (2.3)
$CC_{1/2}$	0.998 (0.685)	0.991 (0.750)	0.959 (0.321)	0.890 (0.881)
Completeness	0.99 (0.87)	0.99 (1.00)	0.96 (0.77)	0.98 (0.92)
Redundancy	6.7 (1.6)	8.1 (6.0)	4.6 (4.0)	3.8 (3.8)
Refinement				
Resolution (Å)	17.5 – 1.80	17.7 – 2.34	37.9 – 2.62	39.0 – 2.98
Unique reflections	76417	34537	23997	16139
$R_{\text{work}} / R_{\text{free}}$	0.19/0.21	0.20/0.22	0.20/0.24	0.23/0.26
No. atoms	4239	3597	3446	3190
Protein	3623	3167	3371	3109
Ligand/ion	15	39	30	55
Water	601	391	45	26
<i>B</i> factors				
Protein	20.7	28.3	65.8	57.2
Ligand/ion	41.0	46.4	100.8	84.2
Water	33.3	37.8	56.6	47.9
R.m.s. deviations				
Bond lengths (Å)	0.015	0.002	0.004	0.002
Bond angles (°)	1.17	0.478	0.604	0.512
PDB ID	6BSQ	6BSR		

^a Values in parentheses are for highest-resolution shell.

Table 3: DSF T_m values for free and acylated PBP4 and PBP5

PBP	1 hr incubation		12 hr incubation	
	T_m (°C)	ΔT_m (°C)	T_m (°C)	ΔT_m (°C)
PBP4				
apo	54.4 ± 0.0	--	53.4 ± 0.2	--
benzylpenicillin	53.6 ± 0.0	- 0.8	53.0 ± 0.1	- 0.4
imipenem	54.9 ± 0.2	+ 0.5	55.2 ± 0.0	+ 1.8
ceftaroline	50.8 ± 0.1	- 3.6	51.4 ± 0.0	- 2.0
PBP5				
apo	53.2 ± 0.0	--	53.0 ± 0.0	--
benzylpenicillin	53.9 ± 0.3	+ 0.7	54.8 ± 0.2	+ 1.8
imipenem	53.5 ± 0.2	+ 0.3	53.2 ± 0.3	+ 0.2
ceftaroline	56.4 ± 0.0	+ 3.2	57.2 ± 03	+ 4.2

Figure Captions.

Figure 1. Key elements of PBP transpeptidase (TP) domains. *Left*, surface representation of the PBP5 active site cleft, with the location of the catalytic serine highlighted in red. *Right*, the key conserved motifs of the PBP TP domains, including motif I, which includes the catalytic serine (SxxK, red), motif II (NxS, mint), motif III (KTGT/S, purple) and the lid (yellow-green), which sits covers that active site to form the deep cleft seen at the right.

Figure 2. PBP4 and PBP5 contain four distinct domains whose topologies are highly interconnected. **A.** The closed (left) and open (right) conformations of *E. faecium* PBP5, colored by domain (N1, dark blue, N2, light blue, non-penicillin binding (nBP), beige, and transpeptidase (TP), orange). The rotations of the N1 and N2 domains relative to the nBP/TP domains, which results in a 24 Å opening of the cleft, are indicated, with the locations of the hinges shown as a dashed box. The location of catalytic Ser422 is indicated by an arrow. **B.** The structure of *E. faecalis* PBP4 colored as in A. No interpretable electron density was observed for the N1 domain and it presumed to be dynamic; it is illustrated here as a cartoon. **C.** Secondary structure and topology map of PBP5. Colors from the N-to-C terminus are indicated next to the structure.

Figure 3. The N1 and N2 domains of the low-affinity subclass of class B PBPs are highly dynamic. **A.** *Left*, superposition of PBP5_{fm} (open, purple), PBP5_{fm} (closed, pink), PBP4_{fs} (cyan) and PBP2a_{Sa} (grey) using their respective TP domains. The N1 and N2 domains of are highlighted in light blue and light purple, respectively. *Right*, the magnitude of the rotations observed between the various N1 (light blue) and N2 (light purple) domains are indicated. *Inset*, cartoon of the PBP domains, with the N1 and N2 domains shown as dashed lines with arrows to highlight their ability to rotated freely of one another. **B.** Superposition of the N1 domains from PBP5 (purple), PBP2a (grey) and the ketosteroid isomerase-like protein from *P. atrosepticum*

(PDBID 3D9R, yellow). **C.** Superposition of the N2 domains from PBP5 (purple), PBP4 (cyan), PBP2a (grey) and ATP-dependent CLP protease adaptor protein CLPS2 (PDBID 4YJM, beige).

Figure 4. β -lactam adduct formation results in similar, but distinct sets of conformational changes at the PBP4 TP catalytic cleft. **A.** *Left*, the structure of benzylpenicillin. *Right*, the XXX electron density (contoured at $X\sigma$ to X resolution; upper right) for the benzylpenicillin acylated Ser424. **B.** *Left*, the structure of imipenem. *Right*, the XXX electron density (contoured at $X\sigma$ to X resolution; upper right) for the imipenem acylated Ser424. **C.** *Left*, the structure of ceftaroline. *Right*, the XXX electron density (contoured at $X\sigma$ to X resolution; upper right) for the ceftaroline acylated Ser424. **D.** Active site in the benzylpenicillin-acyl-PBP4 structure (benzylpenicillin, green; PBP4, light blue; Ser424, pink). Polar interactions are indicated by dashed lines. **E.** *Left*, surface representation of PBP4 (light blue) with bound benzylpenicillin (green). *Right*, overlay of non-acylated PBP4 (cyan) with benzylpenicillin-acyl-PBP4 (light blue; acylated Ser424, pink; view rotated by 90° compared to that in 'D'). Conformational changes in backbone and side chain atoms highlighted with arrows. *Bottom*, overlay orientation same as that in 'D', highlighting opening of the lid to accommodate benzylpenicillin binding. **F.** Active site in the imipenem-acyl-PBP4 structure (imipenem, orange; PBP4, blue; Ser424, pink). Polar interactions are indicated by dashed lines. **G.** *Left*, surface representation of PBP4 (blue) with bound imipenem (orange). *Right*, overlay of non-acylated PBP4 (cyan) with imipenem-acyl-PBP4 (blue; acylated Ser424, pink; view rotated by 90° compared to that in 'D'). Conformational changes in backbone and side chain atoms highlighted with arrows. *Bottom*, overlay orientation same as that in 'D', highlighting opening of the lid to accommodate imipenem binding. **H.** Active site in the ceftaroline-acyl-PBP4 structure (ceftaroline, yellow; PBP4, dark blue; Ser424, pink). Polar interactions are indicated by dashed lines. **I.** *Left*, surface representation of PBP4 (dark blue) with bound ceftaroline (yellow). *Right*, overlay of non-acylated PBP4 (cyan) with ceftarolin-acyl-PBP4 (blue; acylated Ser424, pink; view

rotated by 90° compared to that in 'D'. Conformational changes in backbone and side chain atoms highlighted with arrows. *Bottom*, overlay orientation same as that in 'D', highlighting opening of the lid to accommodate ceftaroline binding.

Figure 1

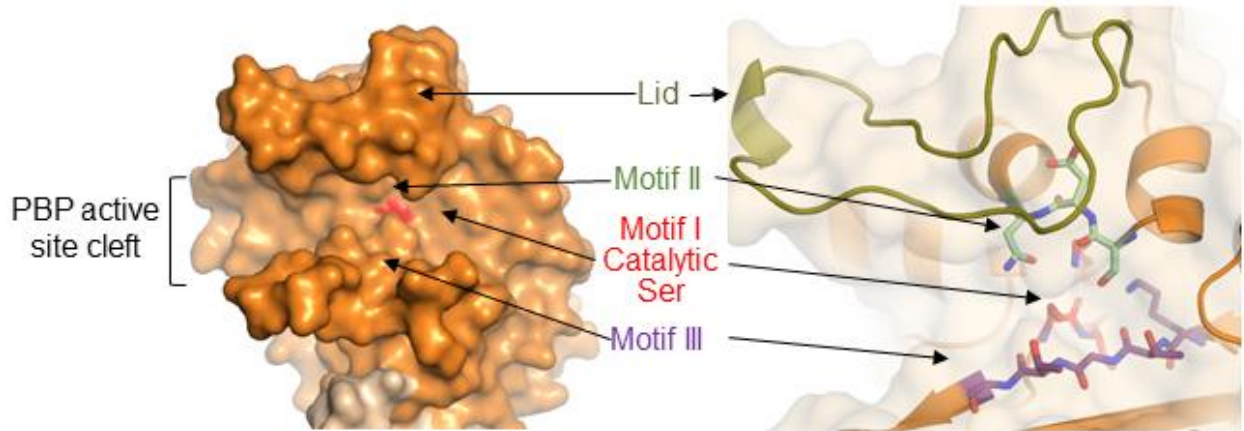


Figure 2

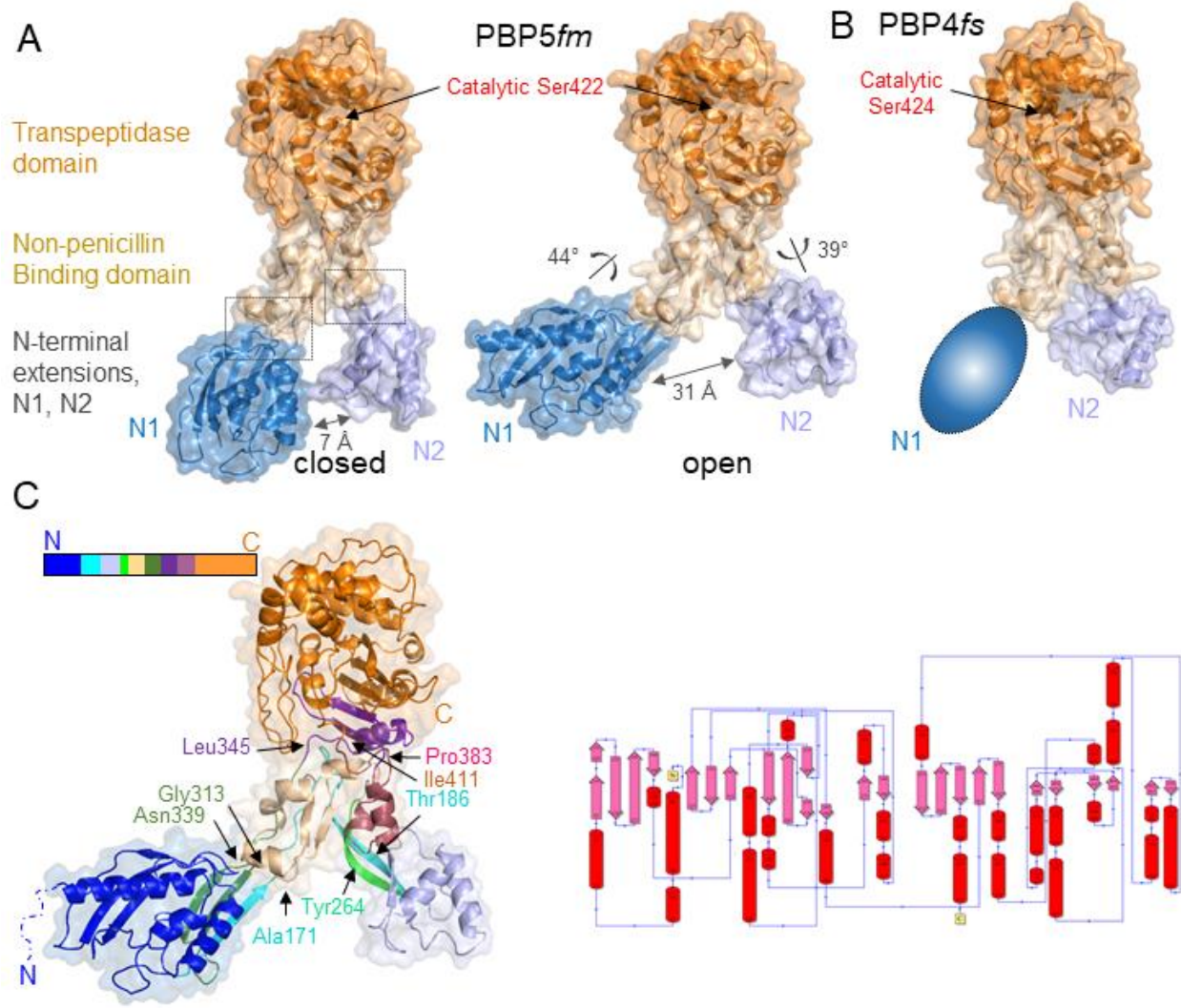


Figure 3

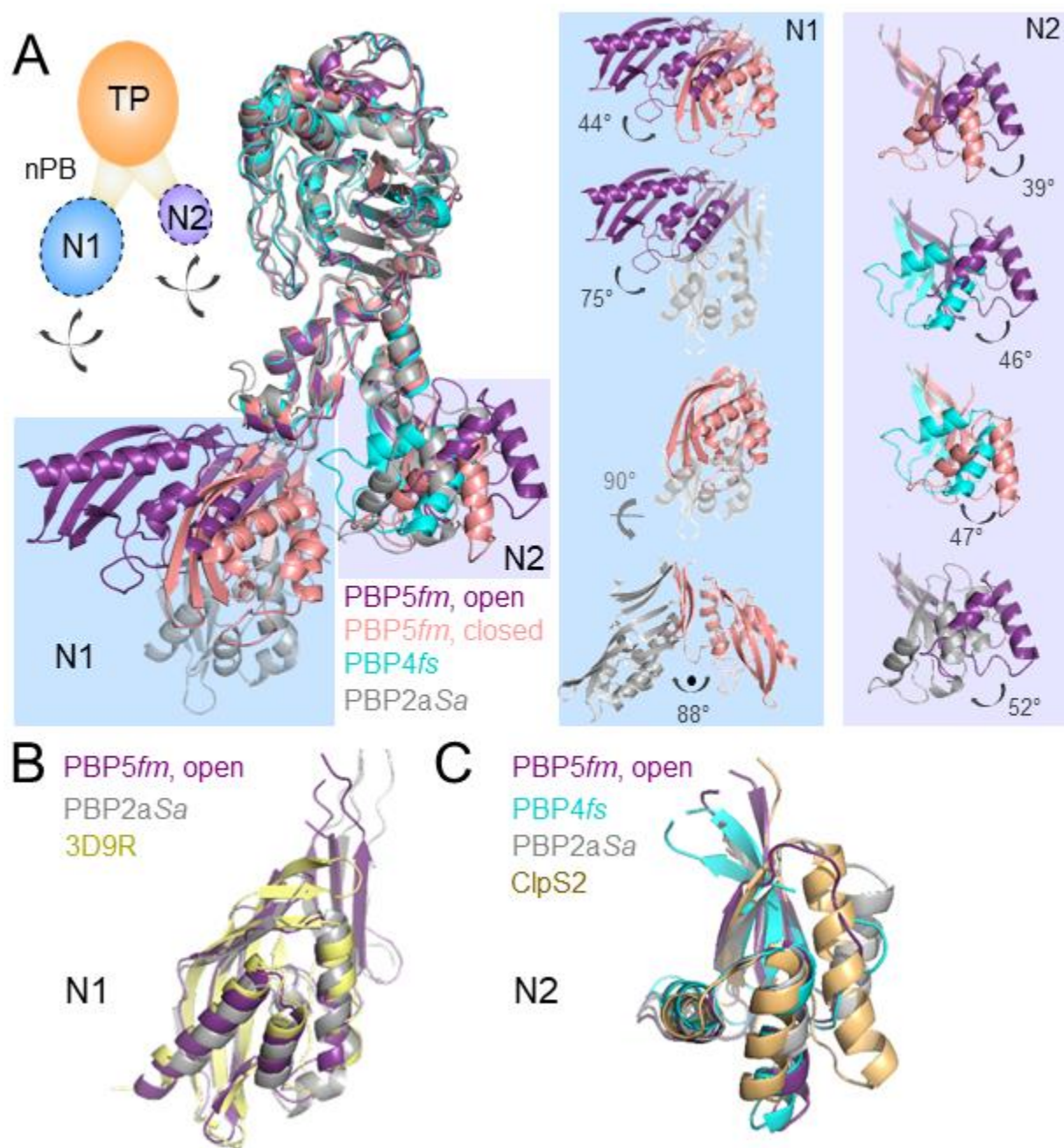
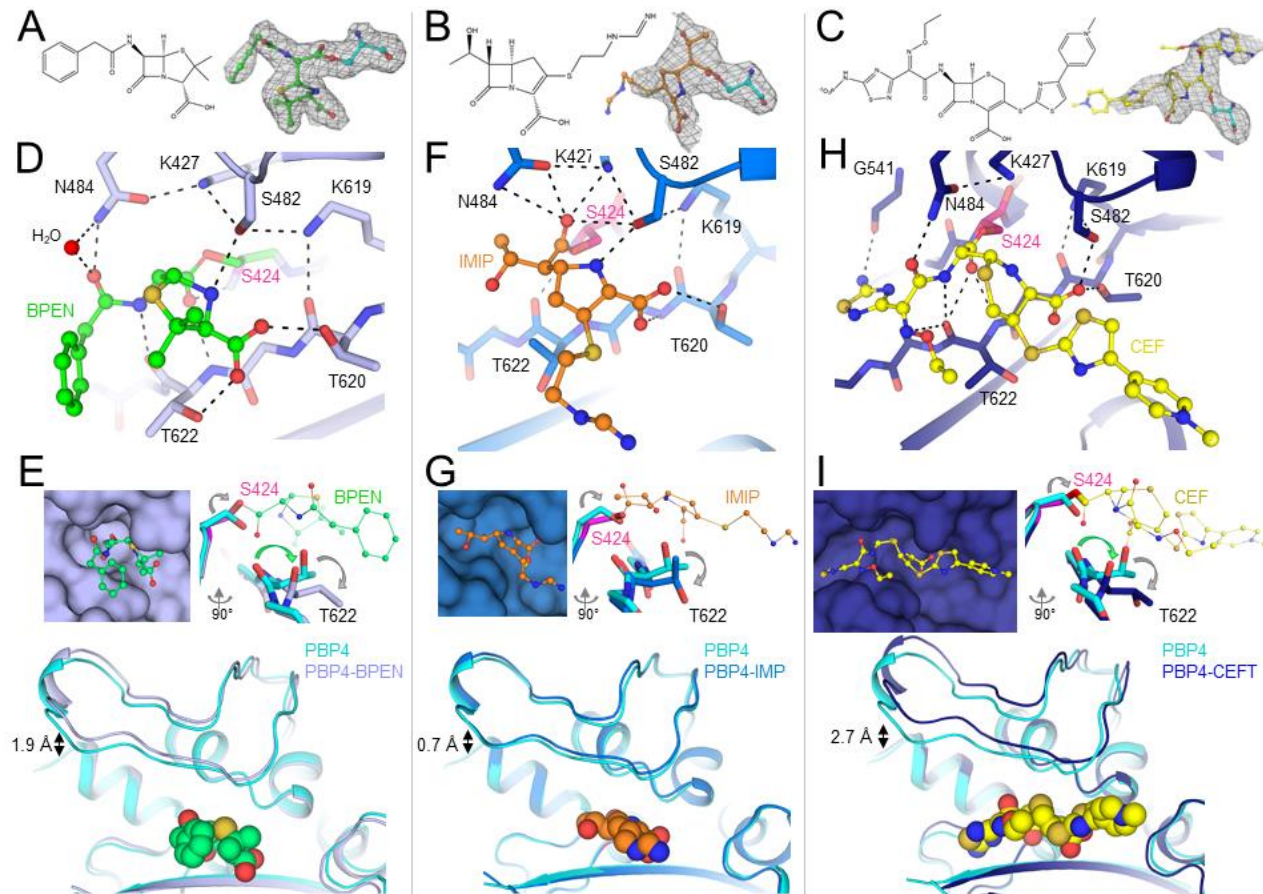


Figure 4



1. **Rice, L. B.** 2008. Federal funding for the study of antimicrobial resistance in nosocomial pathogens: no ESKAPE. *J Infect Dis* **197**:1079-81.
2. **Weiner, L. M., A. K. Webb, B. Limbago, M. A. Dudeck, J. Patel, A. J. Kallen, J. R. Edwards, and D. M. Sievert.** 2016. Antimicrobial-Resistant Pathogens Associated With Healthcare-Associated Infections: Summary of Data Reported to the National Healthcare Safety Network at the Centers for Disease Control and Prevention, 2011-2014. *Infect Control Hosp Epidemiol* **37**:1288-1301.
3. **Arias, C. A., and B. E. Murray.** 2012. The rise of the Enterococcus: beyond vancomycin resistance. *Nat Rev Microbiol* **10**:266-78.
4. **Moellering, R. C., and A. N. Weinberg.** 1971. Studies on antibiotic synergism against enterococci. II. Effect of various antibiotics on the uptake of ¹⁴C-labelled streptomycin by enterococci. *Journal of Clinical Investigation* **50**:2580-2584.
5. **Jawetz, E., and M. Sonne.** 1966. Penicillin-streptomycin treatment of enterococcal endocarditis: a reevaluation. *New England Journal of Medicine* **274**:710-715.
6. **Williamson, R., S. B. Calderwood, R. C. J. Moellering, and A. Tomasz.** 1983. Studies on the mechanism of intrinsic resistance to β -lactam antibiotic in Group D streptococci. *Journal of General Microbiology* **129**:813-822.

7. **Williamson, R., C. LaBouguenec, L. Gutmann, and T. Horaud.** 1985. One or two low affinity penicillin-binding proteins may be responsible for the range of susceptibility of *Enterococcus faecium* to penicillin. *Journal of General Microbiology* **131**:1933-1940.
8. **Rice, L. B., S. Bellais, L. L. Carias, R. Hutton-Thomas, R. A. Bonomo, P. Caspers, M. G. Page, and L. Gutmann.** 2004. Impact of specific pbp5 mutations on expression of beta-lactam resistance in *Enterococcus faecium*. *Antimicrob Agents Chemother* **48**:3028-32.
9. **Rice, L. B., C. Desbonnet, A. Tait-Kamradt, M. Garcia-Solache, J. Lonks, T. M. Moon, E. D. D'Andrea, R. Page, and W. Peti.** 2018. Structural and Regulatory Changes in PBP4 Trigger Decreased beta-Lactam Susceptibility in *Enterococcus faecalis*. *MBio* **9**.